Supplementary Information for

Rapid and Orthogonal Logic Gating with a Gibberellin-induced Dimerization System

Authors:

Takafumi Miyamoto[1]*, Robert DeRose[1]*, Allison Suarez[1], Tasuku Ueno[1], Melinda Chen[1], Tai-ping Sun[2], Michael J. Wolfgang[3], Chandrani Mukherjee[4], David J. Meyers[4] and Takanari Inoue[1†]

(*Equal contribution)

Affiliations:

[1]Department of Cell Biology, Center for Cell Dynamics

[2]Department of Biology, Duke University, Durham, NC 27708

[3]Department of Biological Chemistry

[4]Department of Pharmacology and Molecular Sciences, Synthetic Core Facility,

[1,3,4]School of Medicine, Johns Hopkins University, Baltimore, MD, 21205

[†]To Whom Correspondence Should be Addressed:

Takanari Inoue, PhD.

Phone: 1-443-287-7668

Fax: 1-410-614-8375

E-mail: jctinoue@jhmi.edu

Supplementary Methods

Synthesis of GA_3 acetoxymethyl ester (GA_3-AM)

Supplementary Scheme 1.

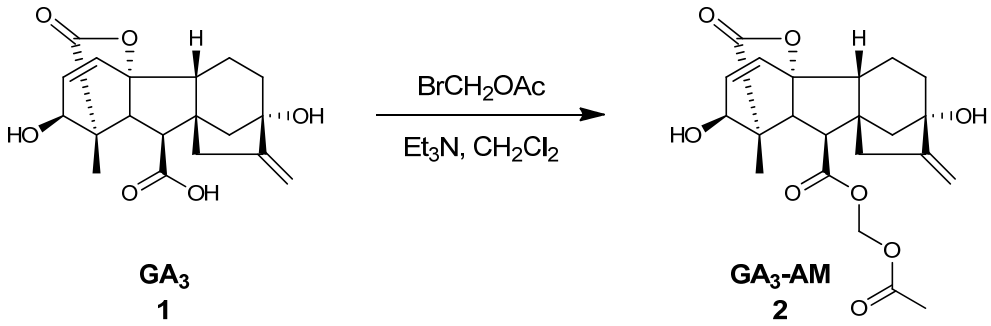

The acetoxymethyl ester of gibberellic acid (GA_3, CAS#: 77-06-5, 99% pure, Fisher-Acros) (**1**) was synthesized following a procedure reported in literature (Supplementary reference 5). To a suspension of GA_3 (0.12 g, 0.35 mmol) in anhydrous dichloromethane (10 ml) under argon was added triethylamine (0.07 ml, 0.52 mmol) dropwise followed by bromomethylacetate (0.04 ml, 0.42 mmol (CAS#: 590-97-6, 98% pure, Fisher-Acros). The resulting mixture was stirred at room temperature for 8 h. The reaction mixture was concentrated under vacuum, and the product was purified using flash chromatography (4 g silica gel cartridge column, 0-8% methanol/ethyl acetate gradient) to yield a colorless solid (0.14 g, 70%), GA_3-AM (**2**); ^{1}H NMR (400 MHz, CD_3OD): δ 1.13 (s, 3H), 1.69-1.98 (m, 8H), 2.04 (s, 3H), 2.20 (s, 2H), 2.72 (d, *J* = 12.0 Hz, 1H), 3.21-3.27 (m, 2H), 3.96 (s, 1H), 4.91 (s, 1H), 5.18 (s, 1H), 5.72 (d, *J* = 4.0 Hz, 1H), 5.79 (d, *J* = 8.0 Hz, 1H), 5.83 and 5.85 (dd, *J* = 4.0 and 8.0 Hz, 1H), 6.33 (d, *J* = 8.0 Hz, 1H); ^{13}C NMR (100 MHz, CD_3OD): δ 15.00, 17.91, 20.53, 39.72, 43.83, 45.32, 51.57, 51.84, 52.35, 53.87, 54.89, 70.43, 78.47, 80.51, 92.17, 107.70, 133.14, 134.05, 158.03, 170.92, 172.14, 180.58; HRMS (*m/z*): $[M+Na]^+$ calcd for $C_{22}H_{26}O_8Na$, 441.1525; found, 441.1527.

Synthesis of GA_3-hydroxamate (GA_3-H)

Supplementary Scheme 2.

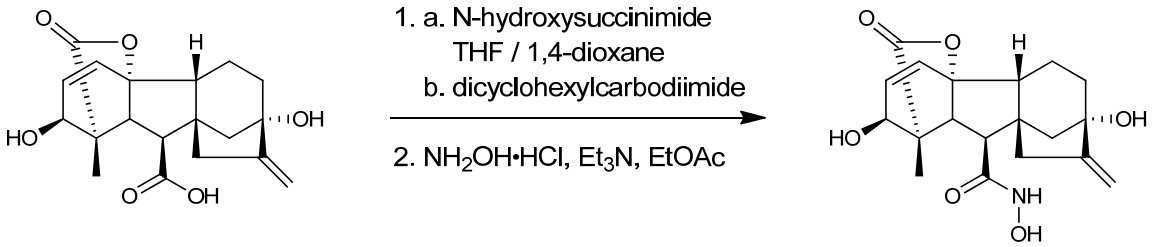

GA_3
1

GA_3-H
3

The hydroxamate of gibberellic acid (GA_3) (**1**) was synthesized following a procedure reported in literature (Supplementary reference 6). To a mixture of GA_3 (0.15 g, 0.043 mmol) and N-hydroxysuccinimide (0.050 g, 0.043 mmol) in anhydrous THF:dioxane (1:1, 20.0 ml) under argon at -10 °C was added a solution of dicyclohexylcarbodiimide (0.11 g, 0.051 mmol) in anhydrous THF:dioxane (1:1, 10.0 ml). The resulting mixture was stirred at -10 °C for 2 h and then at room temperature for 16 h. After filtration of precipitated dicyclohexylurea, the reaction mixture was concentrated under vacuum and the product was purified using flash chromatography (4 g silica gel cartridge column, 0-10% methanol/dichloromethane gradient) to yield succinimidyl gibberellate as a colorless solid (0.19 g, 100%). Data for the succinimidyl gibberellate was in agreement to that found in the literature (Supplementary reference 6).

To a stirred solution of hydroxylamine hydrochloride (0.030 g, 0.044 mmol) and triethylamine (0.11 ml, 0.08 mmol) in EtOAc (35.0 ml) succinimidyl gibberellate (0.19 g) dissolved in EtOAc (30 ml) was added. The reaction mixture was stirred at room temperature for 24 h. After addition of ethanol (12 ml) to dissolve the precipitate, the reaction mixture was stirred at room temperature for another 48 h. The reaction mixture was concentrated under vacuum and the product was purified using reverse phase flash chromatography (4 g C18 cartridge column, 0-100% acetonitrile/water gradient) to yield GA_3-hydroxamate (GA_3-H) (**3**) as a colorless solid (0.13 g, 87%). ^{1}H NMR (400 MHz, DMSO-d_6): δ 1.06 (s, 3H), 1.49-1.65 (m, 5H), 1.82-1.88 (m, 2H), 2.06-2.16 (m, 2H), 2.33 (d, *J* = 12.0 Hz, 1H), 3.12 (d, *J* = 12.0 Hz, 1H), 3.84 (s, 1H), 4.78 and 4.82 (s, 1H each), 5.06 (s, 1H), 5.53 (s, 1H), 5.76 and 5.78 (dd, *J* = 4.0 and 8.0 Hz, 1H),

6.32 (d, *J* = 12.0 Hz, 1H), 8.92 (brs, 1H), 10.54 (brs, 1H); ^{13}C NMR (100 MHz, DMSO-d_6): δ 14.38, 16.66, 43.24, 44.81, 45.59, 48.59, 49.75, 50.39, 52.10, 53.19, 68.64, 76.85, 91.06, 105.44, 131.51, 133.38, 157.91, 167.63, 179.11; HRMS (*m/z*): $[M+NH_4]^+$ calcd for $C_{19}H_{27}N_2O_6$, 379.1864; found, 379.1855.

DNA construction

For YFP-GID1 and GFP-GID1, a PCR product encoding *Arabidopsis thaliana* GID1 (Supplementary Reference 7) was digested using BsrGI and SacI, and then inserted into the multiple cloning site of the pEYFP-C1 or pEGFP-C1 vector (Clontech), respectively.

For CFP-GAI(1-92), (1-151), (1-172), and full length (1-532), PCR products encoding full length and C-terminally truncated *Arabidopsis thaliana* GAI (Supplementary Reference 8) were individually digested using BsrGI and SacI, and then inserted into the multiple cloning site of the pECFP-C1 vector (Clontech).

For Lyn-CFP-GAI(1-92), (1-151), (1-172), and full length (1-532), CFP-GAI(1-92), (1-151), (1-172), and full length (1-532) were digested with NheI and BsrGI, and then inserted into Lyn-CFP-FRB (Supplementary Reference 9) that have been digested with the same set of restriction enzymes.

For Lyn-mCherry-GAI(1-92), CFP-GAI(1-92) was digested with NheI and BsrGI, and then inserted into Lyn-mCherry-FRB (Supplementary Reference 9) that has been digested with the same set of restriction enzymes.

For Tom20-mCherry-GAI(1-92), CFP-GAI(1-92) was digested with NheI and BsrGI, and then inserted into Tom20-mCherry-FKBP (Supplementary Reference 9) that has been digested with the same set of restriction enzymes.

For NLS-CFP-GAI(1-92), annealed primers encoding nuclear localization signal (ATGGATCCAAAAAAGAAGAGAAAGGTAGATCCAAAAAAGAAGAGAAAGGTAGATCCAAAA

AAGAAGAGAAAGGTA) was inserted into the CFP-GAI (1-92) which was digested using NheI and AgeI.

For Tiam1-YFP-GID1, a PCR product encoding C-terminal 1740 bp of TIAM1 (Supplementary Reference 10) was digested using AgeI, and then inserted into YFP-GID1 that has been digested with AgeI.

For Lyn-CFP-FRB-GAI(1-92), a PCR product encoding N-terminal 276 bp of GAI was digested using SacI, and then inserted into Lyn-CFP-FRB that has been digested with SacI.

For FKBP-YFP-Tiam1-GID1, FKBP-YFP (Supplementary Reference 10) was digested with NheI and AgeI, and then inserted into YFP-Tiam1-GID that has been digested with the same set of restriction enzymes.

For FKBP-YFP-GID1, FRB-YFP-GID1 was digested with BsrGI + BamHI, and then inserted into FKBP-YFP that has been digested with the same set of restriction enzymes.

Supplementary Results

Supplementary Figure Legends

Supplementary Figure 1. FRET assays to determine rate constants of binding of GAI to GID1 induced by GA_3 or GA_3-AM. CFP-GAI and YFP-GID1 were co-transfected in HeLa cells, and CFP-YFP FRET was recorded before and after addition of GA_3 or GA_3-AM (both at 100 μM). Values represent mean ± SEM (n ≥ 10, from three independent experiments).

Supplementary Figure 2. Truncations of GAI protein to determine minimum domains necessary for CID. (**a**) Schematic diagram of full-length GAI protein and the three truncated versions used in this paper, showing the known domains. The DELLA and VHYNP domains are sufficient for interaction with GID1 in mammalian cells. For complete discussion of all the domains, see Supplementary references 1-4. (**b**) FRET assays to determine rate constants of binding of truncated GAI to GID1. CFP-GAI versions and YFP-GID1 were co-transfected in HeLa cells, and CFP-YFP FRET was recorded upon treatment with GA_3-AM (100 μM). Values represent mean ± SEM (n ≥ 10, from three independent experiments).

Supplementary Figure 3. Expression of truncated GAI constructs in HeLa cells is higher than that of the full-length version. CFP fluorescence for the cells in Supplementary Figure 2b was measured and normalized to that of cells expressing CFP-GAI(1-532). Values represent mean ± SEM (n ≥ 10, from three independent experiments).

Supplementary Figure 4. The gibberellin CID translocation system is functional in different cell types. Confocal fluorescence microscopy images of Lyn-mCherry-GAI(1-92) and YFP-GID1 in

HEK293T, NIH3T3, and MCF10A cells. The images were taken before and 60 seconds after addition of DMSO (left panels) or 10 μM GA_3-AM (right panels). Scale bar indicates 10 μm.

Supplementary Figure 5. Determining translocation rate constants. (**a**) YFP fluorescence intensity in the cytoplasm of a representative cell from the experiment in Figure 1b was plotted as a function of time. (**b**) Translocation rate constants were calculated for varying concentrations of GA_3-AM and GA_3-H. (**c**) Translocation of the truncated GAI versions GAI(1-151) and GAI(1-172). Experiments were performed as in Figure 1b. Values represent mean ± SEM (n ≥ 4, from three independent experiments).

Supplementary Figure 6. Measurement of esterase activity in COS-7 cells. Cells were incubated with calcein-AM (100 μM) for 30 seconds, then washed, and cells were imaged for fluorescence. The cell images shown at the bottom correspond to each time point of the line graph on top. Values represent mean ± SEM (n=28 cells).

Supplementary Figure 7. GA_3-hydroxamate has weak dimerizing activity compared to GA_3-AM. (**a**) COS-7 cells were co-transfected with CFP-GAI(1-92) and YFP-GID1. FRET signal was measured before and after addition of GA_3-H (1 mM). Plot represents mean of three independent experiments (n=15-20 cells per experiment) ± SEM. (**b**) COS-7 cells were co-transfected with Lyn-mCherry-GAI(1-92) and YFP-GID1 and imaged. GA_3-H (1 mM) was added and induced slow translocation of GFP-GID1 to the plasma membrane. After 510 seconds, GA_3-AM (10 μM) was added and rapidly induced translocation of some remaining cytosolic GFP-GID1 to the plasma membrane.

Supplementary Figure 8. Effect of eserine on GA3-AM-induced protein interaction is concentration dependent. Cell lysate was made as in Figure 1c and eserine added in varying concentrations as shown. GA_3-AM (100 μM) was added, and FRET measured at 0 and 2 minutes. Graph represents the average of three independent experiments ± SEM.

Supplementary Figure 9. Quantitation of the experiment in Figure 2b. Ratio of YFP fluorescence in the nucleus to that in the cytoplasm (relative to that at the start of the experiment) is shown for cells treated with GA_3-AM (10 μM) or DMSO control. Results are shown as the average of three independent experiments (n=20) ± SEM.

Supplementary Figure 10. Epifluorescence microscopy images of NLS-CFP-GAI(1-92) and Inp54p-YFP-GID1 in COS-7 cells. The images were taken before, and 40 and 80 minutes after addition of DMSO or 10 μM GA_3-AM. Scale bar indicates 10 μm.

Supplementary Figure 11. Gibberellin and rapamycin-based CID systems are orthogonal to each other. COS-7 cells were simultaneously co-transfected with Tom20-mCherry-GAI(1-92), Lyn-mCherry-FRB, CFP-FKBP, and YFP-GID1 constructs. Initially, mCherry signal is seen at both plasma membrane and mitochondria, while CFP and YFP are cytoplasmic. Upon simultaneous addition of GA_3-AM and rapamycin (100 μM and 100 nM respectively), CFP-FKBP translocates to the plasma membrane while YFP-GID1 translocates to mitochondria.

Supplementary Figure 12. Effect of gibberellins on intracellular pH. HeLa (**a**) or COS-7 (**b**) cells were co-transfected with CFP and Venus(H148G), whose fluorescence intensity is highly sensitive to small changes in pH. The ratio of YFP to CFP fluorescence (normalized to 1

immediately before addition of drug) is thus an indicator of intracellular pH. YFP and Venus fluorescence was recorded every 30 seconds. After an initial five minutes to establish a baseline, gibberellin (GA_3 or GA_3-AM) was added to a final concentration of 100 or 333 μM and the cells monitored for 15 minutes. NH_4Cl was then added (50 mM) to rapidly drop the pH to 4 to verify that the Venus(H148G) fluorescence was indeed indicating intracellular pH. Values represent mean ± SEM (n ≥ 10, from three independent experiments).

Supplementary Figure 13. Validation of an OR gate using FRET as the output signal. HeLa cells transfected with Lyn-CFP-FRB-GAI(1-92) and FKBP-YFP-GID1 were treated with DMSO (representing the 0,0 input), rapamycin alone (1,0), GA_3-AM alone (0,1) or rapamycin and GA_3-AM together (1,1) and FRET between CFP and YFP was measured every 15 seconds. Data at 90 seconds after drug addition are shown. FRET was seen to increase only for the inputs expected for an OR gate. Values represent mean ± SEM (n ≥ 10, from three independent experiments).

Supplementary Movie 1.

Time series of confocal fluorescence images of COS-7 cells that were transfected with CFP-FKBP (right panel) and YFP-GID1 (left panel) together with Lyn-mCherry-FRB and Tom20-mCherry-GAI(1-92). Rapamycin and GA_3-AM were sequentially added at 1 min and 6.5 min, respectively. The images were taken every 15 sec.

Supplementary References

1. Pysh, l., Wysocka-Diller, J., Camilleri, C., Bouchez, D., & Benfey, P. The GRAS gene family in Arabidopsis: sequence characterization and basic expression analysis of the *SCARECROW-LIKE* genes. *Plant J*. **18**, 111-119 (1999).
2. Willige, B., Ghosh, S., Nill, C., Zourelidou, M., Dohmann, E., Maier, A., & Schwechheimer, C. The DELLA domain of GA INSENSITIVE mediates the interaction with the GA INSENSITIVE DWARF 1A gibberellin receptor of Arabidopsis. *Plant Cell* **19**, 1209-1220 (2007).
3. Peng, J., Carol, P., Richards, D., King, K., Cowling, R., Murphy, G., & Harberd, N., The Arabidopsis GAI gene defines a signaling pathway that negatively regulates gibberellin responses. *Genes Dev* **11**, 3194-3205 (1997).
4. Silverstone, A., Ciampaglio, G., & Sun, T. The Arabidopsis RGA gene encodes a transcriptional regulator repressing the gibberellin signal transduction pathway. *Plant Cell* **10**, 155-169 (1998).
5. Shimano, M., Nagaoka, H., & Yamada, Y. Synthesis of gibberellin A1, A5, A55, and A60: Metal ammonia reduction of gibberellic acid and its derivatives. *Chem Pharm Bull* **38**, 276-278 (1990).
6. Kolbe, A., Kramell, R., Porzel, A., Schmidt, J., Schneider, G. & Adam, G. Syntheses of dexamethasone conjugates of the phytohormones gibberellin A_3 and 24-epicastasterone. *Collect. Czech. Chem. Commun.* **67**, 103-114 (2002).
7. Griffiths, J. et al. Genetic characterization and functional analysis of the GID1 gibberellin receptors in Arabidopsis. *Plant Cell* **18**, 3399-414 (2006).
8. Dill, A., Thomas, S.G., Hu, J., Steber, C.M. & Sun, T.P. The Arabidopsis F-box protein SLEEPY1 targets gibberellin signaling repressors for gibberellin-induced degradation. *Plant Cell* **16**, 1392-405 (2004).

9. Komatsu T. Kukelyansky I, McCaffery JM, Ueno T, Varela LC & Inoue T. Organelle-specific, rapid induction of molecular activities and membrane tethering. *Nat Methods* **7**, 206-8 (2010).
10. Inoue, T., Heo, W.D., Grimley, J.S., Wandless, T.J. & Meyer, T. An inducible translocation strategy to rapidly activate and inhibit small GTPase signaling pathways. *Nat Methods* **2**, 415-8 (2005).